

**SOURCE CHARACTERIZATION OF GROUND TRUTH QUARRY BLASTS IN ISRAEL  
AND CALIBRATION OF LOCAL STATIONS**

Yefim Gitterman and Avi Shapira

Seismology Division, Geophysical Institute of Israel

Sponsored by the U.S. Department of Defense,  
Defense Threat Reduction Agency

Contract No. DSWA01-97-C-0151

**ABSTRACT**

Four recent calibration ripple-fired explosions at the Arad phosphate quarry in the Negev desert were recorded by the ISN short period (SP) and Broad Band (BB) EIL and MRNI stations. Two accelerometers were also installed in close proximity (a few hundred meters) to the explosions to provide better source characterization. Location coordinates and origin times were known to within  $\pm 50\text{m}$  and  $\pm 20\text{ msec}$ , respectively. The blast pattern parameters were also known. These data constitute calibration shots with Ground Truth category GT0. We analyzed correlation of signal features (in both time and frequency domains) and blast patterns as well as travel time curves.

The explosions were conducted a few hundred meters apart using routine (40 msec for EX. 1 and 2) and specially requested (12 msec for EX. 3 and 80 msec for EX. 4) time delays between borehole rows. Total charge weights were 8.0, 10.5, 14.3 and 12.0 tons. The results of the preliminary analysis can be summarized as follows:

1. The yield of EX. 3 was only 19% more than EX. 4; however, it produced far more seismic energy. We attribute this to the shorter delay times in the detonation process. The peak amplitude ratio for the two explosions showed a factor of 2 at short distances (e.g. SP MZDA,  $r=28\text{ km}$ ), increasing with distance to 3 at remote stations (e.g. BB EIL,  $r=161\text{ km}$ ). Similar to EX. 4 amplitudes are observed for EX. 1 and 2 that had much lower yields.
2. The spectral curves show a distinct low-frequency spectral modulation, coherent at different ISN stations. We observed a number of outstanding interference features such as the first null at 5.2 Hz for EX. 1 and the strong main maximum at 14.5 Hz corresponding to the largest time delay in EX. 4.
3. Spectral discriminants, namely Energy Ratio (1-3 Hz/6-8 Hz) and Semblance (1-12 Hz), averaged for a number of ISN stations or for three components of the BB EIL station, showed similar results corresponding to the explosion population. Relatively low ISN ratios and semblance values for EX. 4 could be the result of interference suppression of low frequency energy due to large time delays.
4. High-frequency wave features, which are not available on seismic station recordings, were observed in close-in accelerograms. The strong motion records provided data for the radiation pattern analysis and design of planned larger calibration quarry shots.
5. Observed travel time curves for stations in the 30-250 km range demonstrate a regular time shift of about +2 sec relative to the IASPEI91 model up to 180 km. Far better results were obtained for a local model used by GII for earthquake location where tie residuals do not exceed  $\pm 0.5\text{ sec}$ . We identified an outlying station (SP HRI at 240 km) with a lag of about 1 sec.

The data obtained provide the basis for station correction and improvement of crust models used in the region, and contribute to calibration of two auxiliary IMS stations EIL and MRNI.

**Key Words:** ground truth GT0 quarry blasts, interference phenomena, spectral discrimination, travel time calibration

Table 1. Parameters of controlled ripple-fired quarry blasts in Israel (Hole diameter 200 mm, hole depth 8.5-9 m).

Location and origin time data provided by GPS. O.T. refers to the measured detonation time of the first hole.

#	Date	Origin time (O.T.), GMT	Coordinates	Total yield, tons	Delay, msec		No. of del.	No. of rows	No. of holes	Comments
					Nominal	Real				
1	30.07 1998	08:18:51.91	31.10439N 35.18801E	8	40	32	5	6	70	Nearly-regular blast pattern, almost equal rows (9, 13, 14, 13, 13, 8 holes)
2	09.09 1998	10:00:03.22	31.10416N 35.18880E	10.5	40	31.3	8 (7)	9 (8)	75	Non-regular pattern with variable row length (1-15 holes)
3	26.01 1999	11:46:02.41	31.10968N 35.18914E	14.34	12	-	10	11	120	Non-regular pattern with variable row length (4-13 holes)
4	27.01 1999	10:01:00.64	31.10894N 35.18936E	12.0	80	68.5	9	10	76	Non-regular pattern with variable row length (3-9 holes)

Table 2. Local magnitudes and peak amplitudes of the analyzed quarry blasts.

No. of expl.	Mag. $M_L$	Vertical peak amplitudes at different stations, micron/sec					
		MZDA r=28 km north	YTIR r=29 km north	YASH r=170 km south	HRI r=245 km north	BB EIL r=161 km south	BB MRN r=212 km north
1	2.6	6.2	9.7	0.59	0.57	0.127	-
2	2.7	11.2	8.5	0.79	0.40	0.122	-
3	2.9	17.9	19.6	3.08	2.04	0.389	0.541
4	2.7	8.5	7.8	1.26	-	0.135	0.217

Table 3. Waveform correlation of the quarry blasts at different stations (relatively to EX.1).

Station	Distance, km	Azimuth, deg	Time window, sec	Maximum of the cross-correlation function				Comments
				EX.1	EX.2	EX.3	EX.4	
MZDA	29	35	20	1	0.64	0.32	0.42	-
			35	1	0.63	0.31	0.40	whole signal
YTIR	31	348	10	1	0.39	0.43	0.33	P-waves
			35	1	0.81	0.52	0.37	whole signal
PRNI	84	192	64	1	0.73	0.48	0.61	
			15	1	0.42	0.20	0.20	P-waves
SAGI	110	206	35	1	0.28	0.17	0.25	whole signal
MBH	146	190	45	1	0.55	0.20	0.18	
			15	1	0.61	0.44	0.38	P-waves
			15	1	0.49	0.24	0.20	S-waves
YASH	170	190	15	1	0.41	0.14	0.14	P-waves
			40	1	0.34	0.30	0.22	whole signal

## **OBJECTIVE**

Our research program is aimed at improving monitoring of the CTBT in the Middle East. An important part of the research is the execution and analysis of calibration explosions, currently lacking in the region, including controlled quarry blasts with Ground Truth Information of rank GT0. The data obtained recently are used in the following analysis:

1. An improved understanding of quarry blast phenomenology and characterization of near-field ground motions and waveforms at local and regional distances.
2. Correlation between blast pattern parameters and the amplitude and spectral features of the seismic signal.
3. Discrimination procedures by application of spectral discriminants (semblance and energy ratio) to records of multiple network stations and single BB stations.
4. Travel times and estimation of station corrections for the local and IASPEI91 models.

## **RESEARCH ACCOMPLISHED**

### **Data**

Four routinely-based ripple-fired explosions at the Arad phosphate quarry in the Negev desert were recorded by vertical short period (SP) and 3C Broad Band (BB) stations of the Israel Seismic Network (ISN), at distances of 28-245 km. The stations used in the analysis and the explosion locations are presented on the map in Fig. 1, EIL and MRNI are auxiliary stations of the IMS. The explosions are located a few hundred meters apart, EX.3&4 were adjacent at the same bench. Total charge weights were 8.0, 10.5, 14.3 and 12.0 tons. Routine blasts at this quarry are usually conducted with delays 40 msec between rows of holes (EX.1&2). In the case of EX.3&4 Nonel PETN down-hole delays of 500 ms were used, which can introduce an additional  $\pm 3.5$  msec scatter in the delay times between rows (Rohay, 1999). At our request, two explosions were conducted with blast patterns a little different from routine techniques, i.e. with smaller (12 msec for EX.3) and larger (80 msec, consisting of two 40 msec devices, for EX.4) time delays. These delay values are nominal. As discussed in the following, spectral analysis of seismograms shows that actual quantities were lower. Explosions coordinates and origin times relating to the first blasting hole were measured by GPS with an accuracy better than 50 m and 20 msec, respectively. The summary of the explosion parameters is presented in Table 1. These data constitute calibration shots with Ground Truth category GT0. Two 3C accelerometers (A-800 by Geotech, USA) were also installed in close vicinity of the explosions (within few hundred meters) for better source characterization.

### **Correlation between Blast Parameters and Signal Features**

**Seismic strength.** Local magnitudes based on coda duration measurements and peak amplitudes (as an indication of seismic signal strength) of the analyzed blasts are presented in Table 2. The total yield of EX 3 was only 19% more than that of EX 4, however, it produced far more seismic energy. The peak amplitude ratio for the two explosions showed a factor of 2 at short distances (e.g. MZDA,  $r=28$  km), increasing with distance to 3 at more remote stations (e.g. BB EIL,  $r=161$  km). We attribute this effect to the role of delay times in the detonation process. EX 3 with small delays of 12 msec seems to be similar to that of instantaneous blasting with the strongest seismic effect. EX 4 with large delays of 80 msec decreased seismic energy due to destructive interference phenomenon and corresponds approximately to the one-row blast. The effect of delay times is observed also for EX 1&2 with intermediate delays of 40 msec. These blasts have much lower total yields than EX 4, but produced similar amplitudes. An example of signal amplitude comparison is shown on Fig. 2.

Compared to those of EIL, signal amplitudes for EX 3&4 are enhanced at MRNI, that is located closer at the opposite azimuth (see Table 2, Fig. 1). Such an "azimuth effect" was not observed at the SP stations, e.g. HRI and YASH (see map in Fig. 1 and Table 2). It cannot, therefore, be attributed to the source effect like direction of blast sequencing or orientation and position of the free face; however, it is likely to be associated with path and site effects.

Local duration magnitudes correlate well with peak amplitudes and correspond approximately to the upper limit of the yield-magnitude relationship of ripple-fired quarry blasts (Gitterman, 1998, Khalturin et al., 1998). Records of EX 3 (with delays of 12 msec) are exceptional, as this explosion has a source function more similar to instantaneous blasts.

**Waveform correlation.** We studied waveform correlation from the explosions to check for similarity, i.e., that events from the same mine produce highly repeatable waveforms which, in turn, can be used for event clustering and source identification (e.g. Harris, 1997). Indeed, when comparing normalized seismograms at a specific station (see e.g. Fig. 3), one can observe a conformity in the shape of some phases. Table 3 shows cross-correlation maximal values between EX 1 and the other explosions at several close and remote stations for different time windows. The correlation values decrease significantly with distance (more complicated waveforms and lower signal-to-noise ratio) and increase for larger windows containing the whole wavetrain.

The results demonstrate rather low correlation, although all the blasts were located in a small area of about 0.5 km radius. The highest correlation is between seismograms of EX 1 and EX 2, both having similar blast patterns and delays of 40 msec and spaced about 100 m apart. EX 3&4, with different delays and placed a little further away (500 m), show very low correlation with EX 1, especially at distances greater than 100 km. Similar results were obtained recently by Stump et al. (1999) when regional waveforms from single-fired explosions in a single mine separated by a few kilometers, lost coherency above 1 Hz. All these observations suggest limited applicability of correlation analysis for identifying blasts from a large-scale mine.

**Spectral modulation.** The most characteristic feature of ripple-fired explosions is the spectral modulation in all wave phases (see also Stump and Reinke, 1988, Chapmen et al., 1992, Gitterman and van Eck, 1993). Availability of Ground Truth parameters for the analyzed quarry blasts and relatively simple blast patterns provide a good chance to check the correlation between blast parameters and seismic wave features. We also examine the correspondence between theoretical predictions, based on the linear interference theory, and experiments, for local mining practices and geological settings.

The main ripple-fired source features are explained by constructive (main maximum at  $f_m$ ) and destructive (first spectral null at  $f_{01}$  and multiples  $f_{0k}$ ) interference of seismic waves from inter-shots with millisecond delays (not by source finiteness in space or time, or total blast duration). For a regular blast pattern the frequencies depend on delays  $\tau$ , and number of delays  $n$  (Gitterman, 1982):

$$f_m = 1/\tau \quad (1)$$

$$f_{01} = 1/[(n+1)\times\tau] = f_m/(n+1); \quad f_{0k} = k \times f_{01}, \quad k = 1, 2, \dots, n \quad (2)$$

Any random variation of delay time or charge per delay, or any other non-regularity in the blast pattern not to mention anelastic absorption of high-frequency energy with distance, can destroy the spectral modulation features, most significantly at high frequencies (greater than 10-15 Hz). The spectral null features occur at frequencies lower than the main maximum and so can be useful in identifying ripple-fired quarry blasts at regional distances. Based on numerous observations of quarry blasts in Israel and the simple theoretical analysis mentioned above, we found it better to reveal and analyze spectral modulation at low frequencies (<15 Hz) using smoothed spectra of the whole signal for several stations at different azimuths (Gitterman and van Eck, 1993). Advantage of the low-frequency approach is presented also in Hedlin, 1998, Carr and Garbin, 1998.

Amplitude spectra of the whole signal (20-30 sec window) recorded at different SP and BB stations were smoothed in the 0.5-0.7 Hz window. The spectral shapes showed high coherency and clear modulation (except for EX 3 with too small delays of 12 msec) for all stations including spectral null and main maximum features (Figs. 4-6). According to Eq. (1), EX 4 with delays of  $\tau=80$  msec should produce a main maximum at the frequency  $f_m=12.5$  Hz. Spectral curves at different ISN stations, presented in Fig. 4, show clear modulation and outstanding maximum at 14-15 Hz, highly coherent at different stations (Fig. 4a). From the average spectral curve (Fig. 4b) we estimated an empirical value  $f_m^*=14.6$  Hz. This maximum is rather strong, in spite of: (a) non-regularity of the blast pattern (different number of hole charges in rows), (b) well-known strong attenuation of high-frequency seismic energy in the region ( $Q=50-100$ ) with widespread unconsolidated sediments in the upper crust, and (c) the restricted recording band (0.5-12.5 Hz) at ISN stations. This  $f_m$  feature is first observed for quarry blasts in the region, because existing mining practices in Israel and Jordan usually include delays of  $\tau < 50$  msec. These delays produce main maxima at  $f_m > 20$  Hz which cannot be observed at local seismic stations for reasons (b) and (c) mentioned above. In some geological settings such as shields, e.g. in the eastern USA, with low anelastic absorption, the maxima were observed at frequencies up to 40 Hz (Kim et al., 1994).

The 2Hz-shift of  $f_m$  cannot be explained by a Doppler-like effect caused by specific orientation of detonation between charge rows and azimuth to a station (Chapmen et al., 1992), because the estimate  $f_m^*$  is obtained through averaging of several stations covering the whole azimuth range (see Fig. 1). The most natural reason for the shift is the well-known in mining practices variability of short-time delay systems where actual delays can differ from nominal values by 10-20%. Inverted calculations from Eq. (1) give a reasonable assessment of the actual delay:  $\tau^*=1/f_m^*=68.5$  msec (i.e. about 34 msec on average for a separate delay device which was doubled for this explosion). Moreover, application of the obtained delay for estimation of the first spectral null by Eq. (2), results in a value of  $f_{01}^*=1/[(n+1)\times\tau^*]\approx 1.5$  Hz, which corresponds well to the observed minimum at this frequency on the average spectral curve (Fig. 4b), where the second (2.9 Hz), and the fifth (8 Hz) spectral nulls can also be identified.

In the case of EX. 1 ( $\tau=40$  msec,  $n=5$ ) a distinct first spectral null is observed for ISN stations at  $f_{01}^*=5.2$  Hz (Fig. 5a) as compared to the theoretical value of  $f_{01}=4.2$  Hz in Eq. (2). Supposing reduced (as in the case of EX. 3) delays, we estimated actual values  $\tau^*=1/[(n+1)\times f_{01}^*]\approx 32$  msec. Broad band EIL records (80 Hz sampling rate) from EX. 1 were also analyzed. All three components showed the same LOW-FREQUENCY spectral modulation features (Fig. 5b), and the spectra average corresponds well to the average based on ISN stations. The HIGH-FREQUENCY modulation and the potential main maximum at  $f_m\approx 25-30$  Hz, which could be observed in the band-pass filtered 0.5-40 Hz seismograms, were not found owing to the steep descent of spectra after 10 Hz associated with the above-mentioned local strong attenuation of signal high frequencies. The

modulation features for EX. 2 were also observed in ISN records, but less obvious than for EX. 1 owing to the non-regularity of the blast pattern.

#### **Discrimination Procedures**

Spectral discriminants, namely Energy Ratio of low (1-3 Hz) to high (6-8 Hz) frequency bands and semblance of spectral shapes in (1-12 Hz) band (Gitterman et al., 1996) were applied to seismograms obtained in time windows containing the whole signal. For a given event, the discriminants were averaged for a number of ISN stations (covering a broad azimuth range) or for three components of a single BB station.

Both multi and single station estimates verified the results previously obtained from the Galilee and Negev local data sets (Gitterman et al., 1996): the new controlled quarry blasts also demonstrated higher values of energy ratio and spectral semblance than nearby earthquakes and corresponded to the explosion population (see Table 3). Relatively low energy ratios and semblance values for EX. 4, estimated from ISN records, could be the result of interference suppression of low frequency energy due to large time delays. We found that, for a given explosion, semblance estimates from a single 3C station are higher than those obtained from ISN stations. Such a relation may also be expected for earthquakes. Indeed, for an earthquake from the Galilee dataset (April 15, 1994, 01:20,  $M_L=2.4$ ), a multi-station ISN semblance estimate was 0.45 (see Gitterman et al., 1996), and for the single 3C ISN station ZNT we now obtained a value of 0.776 which is still much lower than for explosions.

#### **Near-Field Observations**

Strong motions for EX 2,3 and 4 were recorded by two A-800 accelerographs at distances of 200-500 m. EX. 3 and EX. 4 yielded approximately equal horizontal Peak Ground Accelerations of 0.3g at about 360 m (Fig. 6a), despite much higher amplitudes and magnitude for EX. 3 at remote seismic stations, as mentioned above. Analysis of the blast patterns and accelerograph locations showed that, for the strong EX. 3, the PGA value was recorded at the free face side in the opposite direction to the detonation sequence, whereas for the weak EX. 4 a sensor was placed along the bench with an azimuth perpendicular to the detonation direction.

Accelerogram spectra demonstrated some high-frequency source features which are not available in seismic station recordings with limited frequency range. Using accelerograms we can observe a main maximum  $f_m \approx 26$  Hz for EX. 1 (Fig. 6b) and multiple main maxima at about 30 Hz and 45 Hz for EX. 4 (Fig. 6c), which could not be found in recordings of ISN stations.

#### **Travel Time Analysis**

Based on the Ground Truth origin times from the controlled quarry blasts and measured first arrival times, we obtained accurate P-waves travel time empirical curves in the 30-250 km range. The curves demonstrate a regular time shift of about +2 sec when compared to the IASPEI91 model, up to 180 km (Fig. 7a). A much better fit is observed with respect to the local model used by GII for earthquake location where the residuals are less than  $\pm 0.5$  sec (Fig. 7b). We identified an outlying station (HRI at Mt. Hermon at 240 km) with a lag of about 1 sec.

#### **CONCLUSIONS AND RECOMMENDATIONS**

The data and results obtained based on Ground Truth information will contribute to a better understanding of ripple-fired quarry blast phenomenology. The observed correlation between blast pattern parameters, waveform amplitudes and spectral features is useful in the identification of seismic events. Using precisely known parameters of actually routine quarry blasts we can predict the basic spectral modulation features and vice-versa from the observed spectra we can estimate actual blast parameters, namely time delays different from nominal values. The application of spectral energy ratio and semblance discriminants to network stations and 3-component BB recordings provided both multi- and single-station estimates relating to the explosion population. Low correlation of near-regional signals from closely spaced routine quarry blasts suggests limited applicability of the waveform correlation analysis or "master event" approach to the discrimination problem. The data obtained provide the basis for station correction and improvement of crust models used in the region and contribute to calibration of two auxiliary IMS stations EIL and MRNI. The strong motion records provided data for design of planned larger calibration quarry shots, including instantaneous explosions.

#### **REFERENCES**

- Carr, D.B and H.D. Garbin, 1998. Discriminating ripple-fired explosions with high-frequency (>16 Hz) data, *Bull. Seis. Soc. Am.*, 88: 963-972.
- Chapman, M.C., G.A. Bollinger, and M.S. Sibol, 1992. Modeling delay-fired explosions spectra at regional distances, *Bull. Seis. Soc. Am.*, 82: 2430-2447.
- Gitterman, Y., 1982. Assessment of dynamic parameters of seismic and air shock waves from multiple shot systems, Ph.D. Thesis, Institute of Mining, Academy of Sciences of the USSR, Novosibirsk.
- Gitterman, Y. and T. van Eck, 1993. Spectra of quarry blasts and microearthquakes recorded at local distances in Israel, *Bull. Seis. Soc. Am.*, 83: 1799-1812.

- Gitterman, Y., 1998. Magnitude yield correlation and amplitude attenuation of chemical explosions in the Middle East. In Proceedings of the 20<sup>th</sup> Annual Seismic Research Symposium on Monitoring a CTBT, 302-311.
- Gitterman, Y., V. Pinsky and A. Shapira, 1996. Discrimination of seismic sources using the Israel Seismic Network, Report No.1, PL-TR-96-2207, 98 pp.
- Hedlin, M.A.H., 1998. Identification of mining blasts at all regional distances using low-frequency seismic signals, in Proceedings of the 20<sup>th</sup> Annual Seismic Research Symposium on Monitoring a CTBT, 335-344.
- Harris, D.B., 1997. Waveform correlation methods for identifying population of calibration events, in Proceedings of the 19<sup>th</sup> Annual Seismic Research Symposium on Monitoring a CTBT, 604-613.
- Khalturin, V., T. Rautian and P. Richards, 1998. The seismic signal strength of chemical explosions, Bull. Seis. Soc. Am., 88, 1511-1524.
- Kim, W.Y., D.W. Simpson and P.G. Richards, 1994. High-frequency spectra of regional phases from earthquakes and chemical explosions, Bull. Seis. Soc. Am., 84, 1365-1386.
- Rohay, A.C., 1999. Modeling ripple fired explosions from the Centralia mine, Southwestern Washington, Abstracts of the 94th Annual Meeting of SSA, Seism. Res. Lett., 70, p.228.
- Stump, B.W. and R.E. Reinke, 1988. Experimental confirmation of superposition from small scale explosions, Bull. Seis. Soc. Am, 78, 1059-1073.
- Stump, B.W., D.C. Pearson and V. Hsu, 1999. Empirical scaling relations for contained single-fired chemical explosions and delay-fired mining explosions at regional distances, Abstracts of the 94th Annual Meeting of SSA, Seism. Res. Lett., 70, p.212.

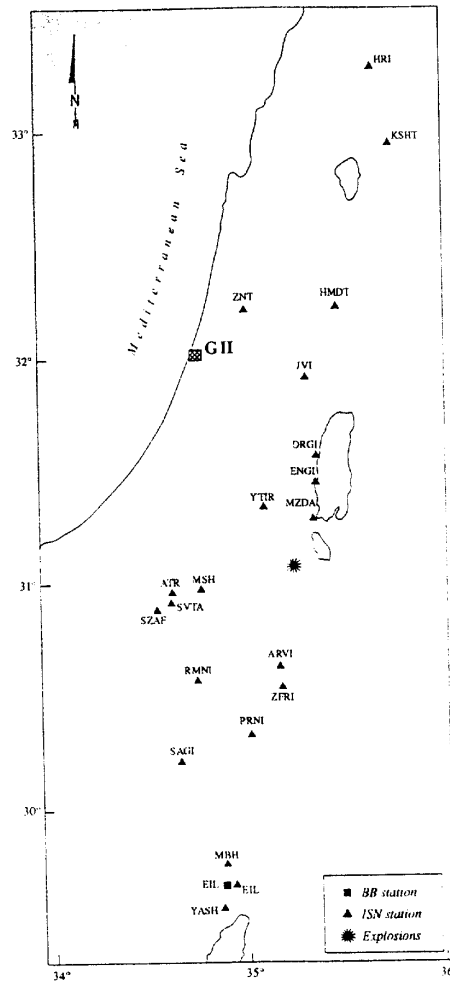


Figure 1. Location of the controlled quarry blasts and seismic stations used in the analysis.

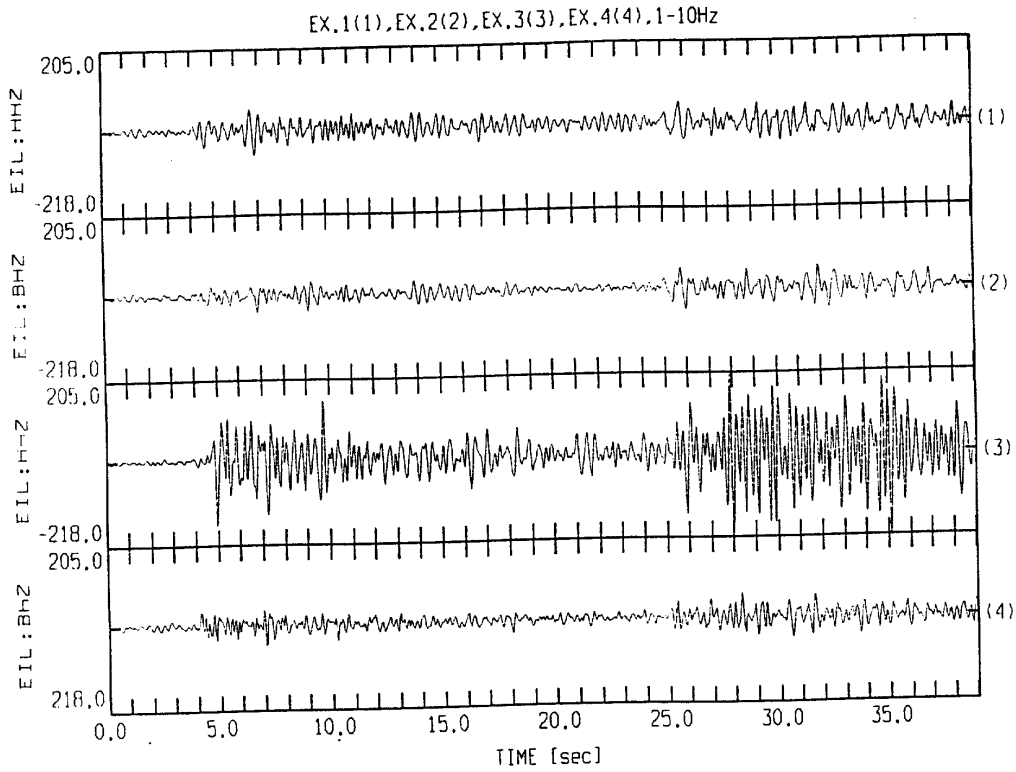


Figure 2. Comparison of amplitudes for the blasts at BB EIL station (vertical component).

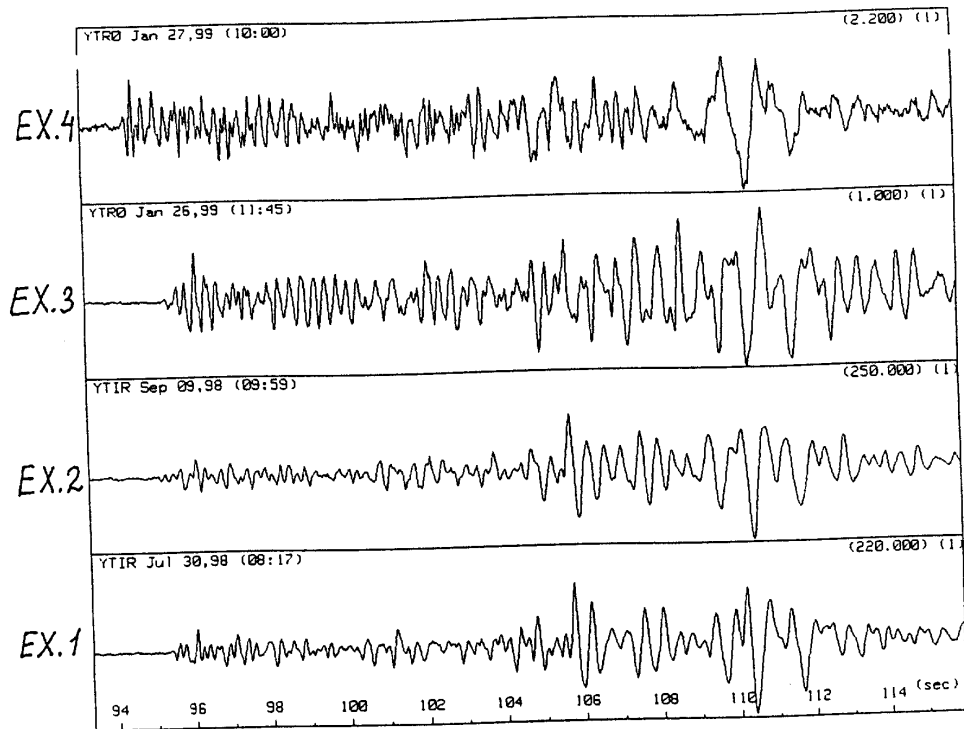


Table 4. Discrimination results for the controlled (calibration) ripple-fired quarry blasts.

No. of expl.	Seismic system	Energy ratio (1-3Hz)/ (6-8Hz)	Semblance in range (1-12 Hz)	Number of stations (ISN), comments
1	SP ISN Vert.	41.0	0.89	11 (ATR, EIL, KER, MBH, MSH, MZDA, PRNI, RMNI, SAGI, YASH, YTIR)
	BB EIL 3C	56.3	0.98	trigger at 80 Hz, filter 0.5-40 Hz
2	SP ISN Vert.	63.3	0.81	11 (DRGI, ENGI, KER, MSH, PRNI, RMNI, RTMM, SVTA, SZAF, YTIR, ZFRI)
	BB EIL 3C	179.4	0.98 (1-10 Hz)	continuous recording at 20 Hz, filter 0.5-10 Hz
3	SP ISN Vert.	15.8	0.78	15 (ATR, DRGI, EIL, ENGI, HMDT, HRI, JVI, MSH, MZDA, PRNI, SAGI, SVTA, SZAF, YASH, ZFRI)
	BB EIL 3C	28.3	0.97	trigger at 80 Hz, filter 0.5-40 Hz
	BB MRN 3C	10.3	0.90 (1-8 Hz)	continuous recording at 20 Hz, filter 0.5-10 Hz
4	SP ISN Vert.	5.6	0.64	9 (ARVI, DSI, MBH, MZDA, PRNI, RMN, SAGI, YASH, YTIR)
	BB EIL 3C	11.2	0.93 (1-8 Hz)	continuous recording at 20 Hz, filter 0.5-10 Hz
	BB MRN 3C	3.9	0.89 (1-8 Hz)	continuous recording at 20 Hz, filter 0.5-10 Hz

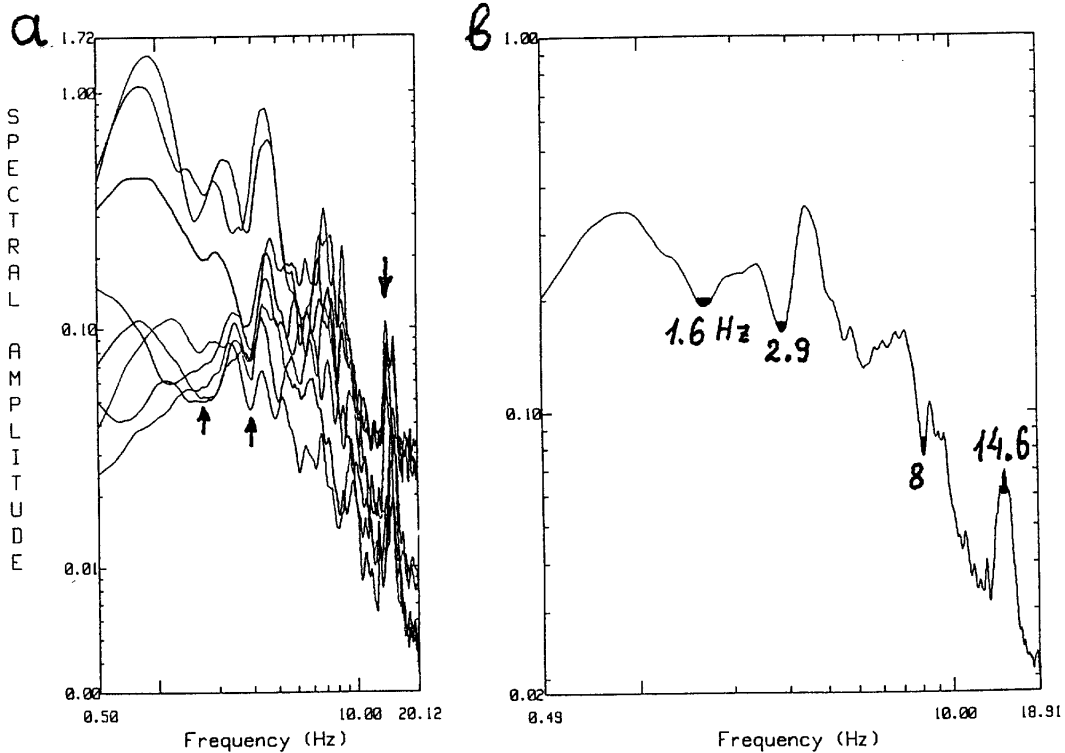


Figure 4. Spectral modulation and the main maximum for EX.4 at ISN stations (a), and the average curve (b).

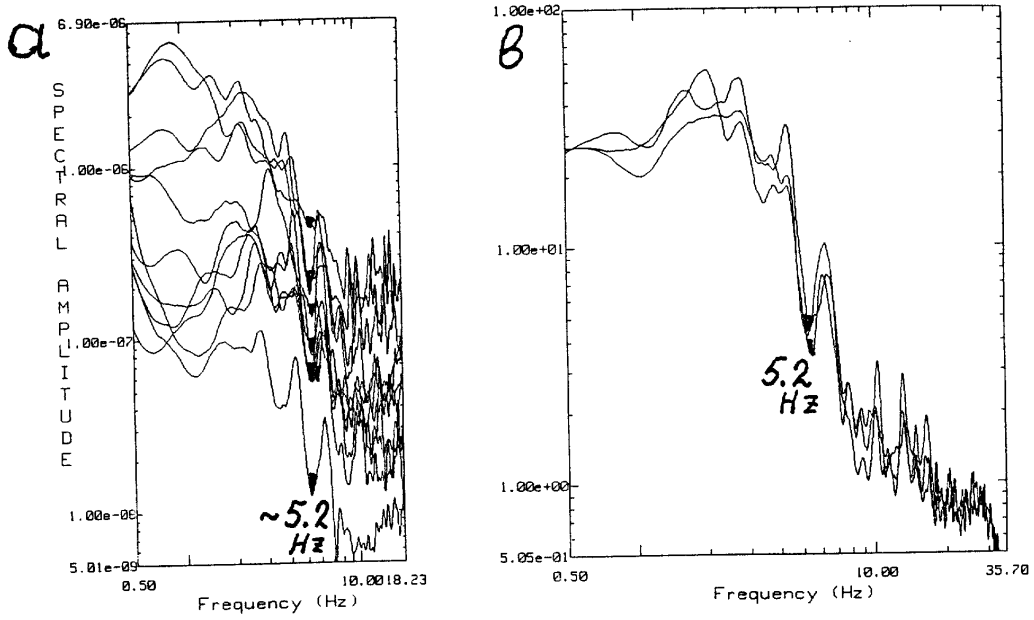


Figure 5. Spectral modulation and the first spectral null feature for EX.1 at ISN stations (a) and at BB EIL 3C station, band-pass filter 0.5-40 Hz (b).

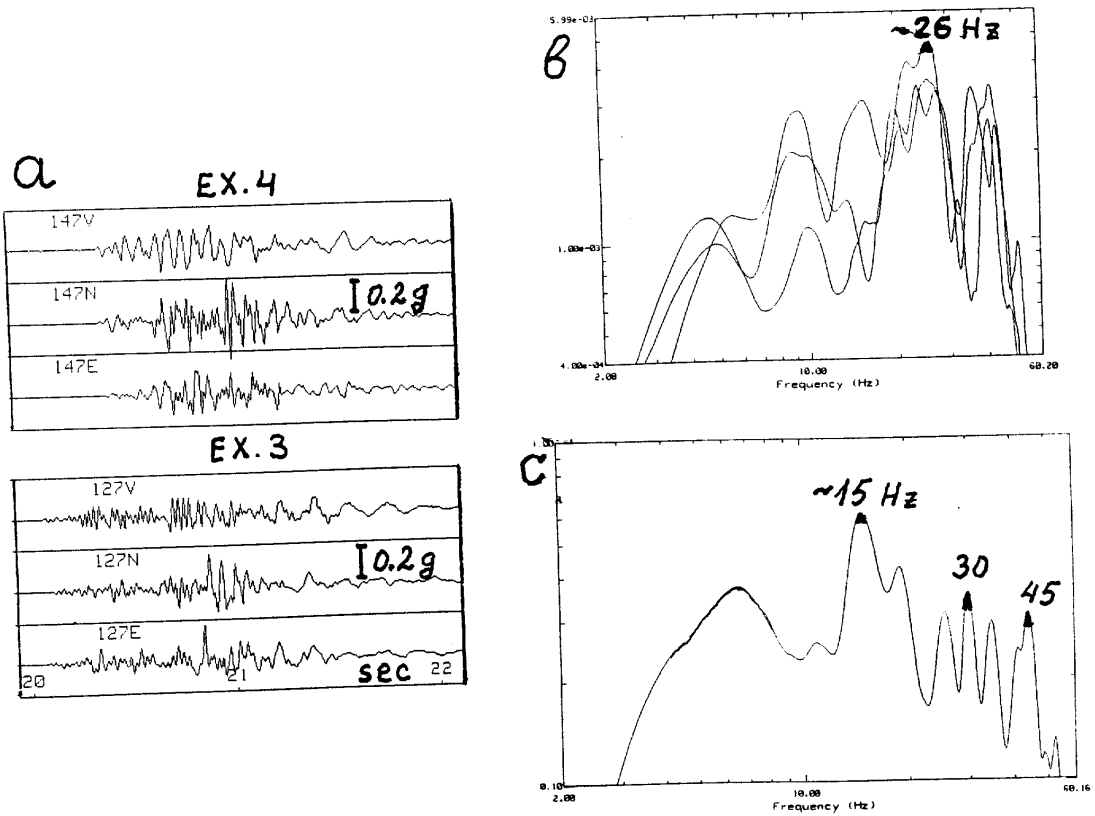
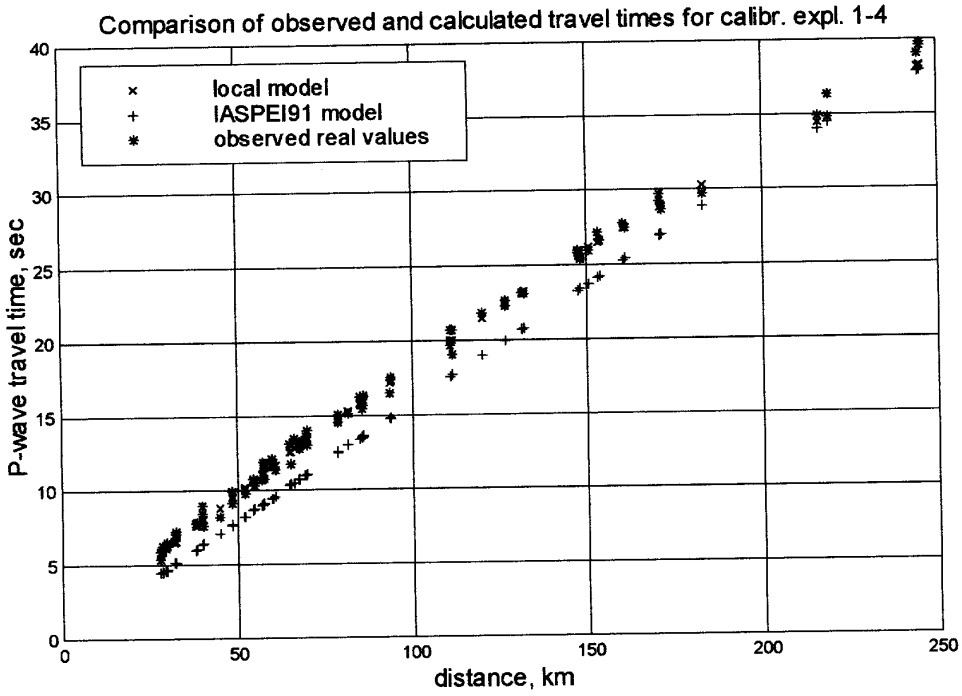


Figure 6. Near-field observations of the blasts: (a) 3-component accelerograms; (b) spectra for EX.2; (c) spectra for EX.3.

**a**



**b**

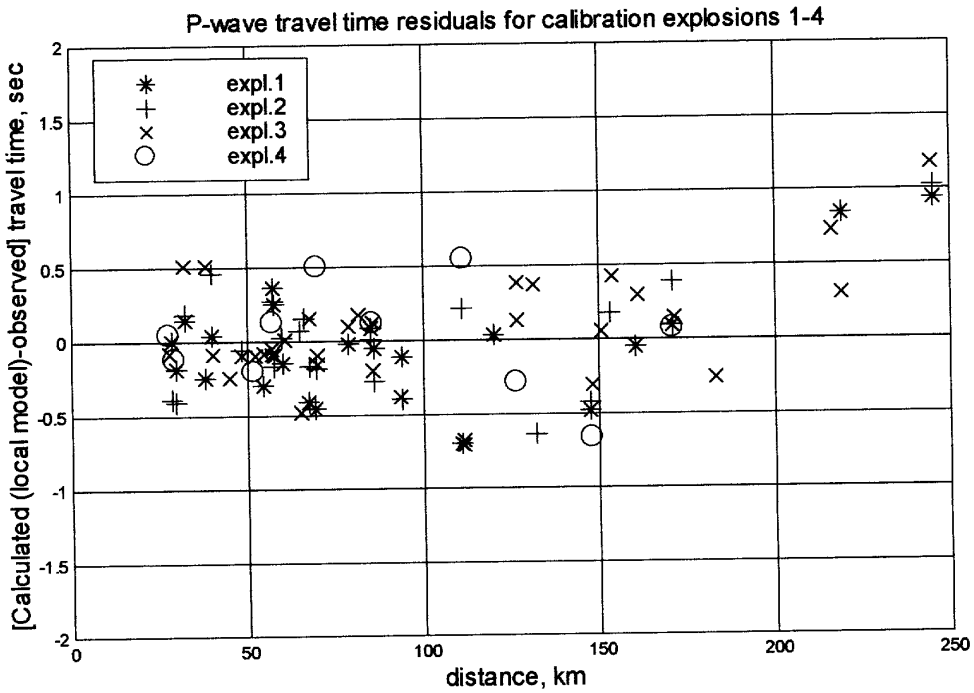


Figure 7. Travel time analysis: (a) observed values for different blasts compared with IASPEI91 and local models; (b) time residuals (observed – calculated) for the local model.